Carpathian Journal of Earth and Environmental Sciences, May 2015, Vol. 10, No. 2, p. 33 - 44

STRUCTURALLY CONTROLLED DEEP HYDROTHERMAL TRANSFORMATION OF ORDOVICIAN CARBONATE RESERVOIRS, CENTRAL TARIM BASIN, NW CHINA

Zhuang RUAN[1], Bingsong YU[1], Jia MA[2] & Yinlu PAN[1]

[1]*State Key Laboratory of Geological Process and Mineral Resources, China University of Geosciences, Beijing 100083, China. Ruanz0103@cugb.edu.cn*

[2]*Beijing Research Institute of Chemical Engineering and Metallurgy, CNNC, Beijing 101149, China.*

Abstract: Ordovician carbonate rock is an important hydrocarbon reservoir in the Tarim Basin of NW China. Secondary reservoir space and cementation are related to deep fluid activity, particularly magmatic hydrothermal fluid. Classification and modeling of the magmatic hydrothermal fluids is important in the identification of high-grade reservoirs. The presence of many anomalously a high-temperature fluid inclusion is indicative of significant hydrothermal activity. Samples from both filling (carbonate or other minerals filled in cracks and dissolution holes of carbonate rocks) and country rocks were collected and their C, O, and Sr isotope ratios analyzed. Filling samples were found to have low $\delta^{13}C$ and $\delta^{18}O$ values, and high $^{87}Sr/^{86}Sr$ values. These samples are distinct from the country rocks and other filling samples, indicating the presence of magmatic hydrothermal fluids. Trace element abundance was analyzed in 11 filling samples, yielding positive Eu anomalies and high Th/U values in some samples. Conduit systems such as unconformities, faults, and cracks limit the distribution of hydrothermal fluid and give it a distinct trace elemental and isotopic signature. The hydrothermal fluid derived from magmatic activity may have caused dissolution, cementation, and an increase in the formation fluid temperature.

Key words: Hydrothermal Fluid, Ordovician Carbonate Reservoir, Tarim Basin, Isotopes, Trace elements

1. INTRODUCTION

Fluid–rock interaction is an integral part of the petroleum system and occurs when fluid from the deep crust or mantle enters the basin, impacting both the porosity and permeability of potential reservoirs. The effects of deep fluid activity on the petroleum system basin are apparent in several aspects: the formation of inorganic gas reservoirs; maturity transformation of the source rock through energy exchange; changing reservoir composition or structure of the rock porosity, thus improving reservoir performance through dissolution or metasomatism; and providing thermal energy, thereby accelerating the process of hydrocarbon migration. Many recent studies of deep fluid activity have focused on thermochemical sulfate reduction (TSR) (Machel & Buschkuehle, 2008; Worden et al., 1996; Worden & Cai, 2006; Zhang et al., 2008), and magmatic hydrothermal fluid dolomitization (Barnes et al., 2008; Davies & Smith, 2006, 2007; Friedman, 2007; Lavoie & Morin, 2004; Lavoie & Chi, 2006) and its role in reservoir formation (Chen et al., 1999; Jin et al., 2004; Kappler & Zeeh, 2003).

The relationship between dolomitization/ dissolution and hydrothermal fluid has been extensively studied (Al-Aasm, 2003; Auajjar & Boulegue, 2002; Guedes et al., 2003; James & Mark 2001; Tritlla et al., 2001). Tritlla et al., (2001) indicated that dolomitization in the lower Triassic limestones of the Espadán Ranges (Iberian Chain, east Spain) was related to a hydrothermal event in the Late Cretaceous. Saddle dolomites in the region yield low $\delta^{18}O$ and $\delta^{13}C$ values. Al-Aasm (2003) also investigated the relationships between fluid flow events and dolomitization in the Western Canada Sedimentary Basin, showing that fluid activity was controlled by faults and that hydrothermal fluids had a strong influence on dolomite formation. Kappler & Zeeh (2000) studied several generations of cemented saddle dolomites in Permian to Tertiary sedimentary rocks in the Southern Alps, showing that dolomitization was related to Late Triassic–Early Jurassic hydrothermal activity along a fault. Jin et al., (2004) investigated the properties of mantle-derived fluids and the rate of hydrocarbon generation in

Liaohe Basin, China, and indicated that mantle-derived fluids have an important effect on hydrocarbon generation by providing both reaction energy and materials.

The Ordovician carbonate reservoir in the Tarim Basin is a typical pore-fractured reservoir that is characterized by a great burial depth and poor initial reservoir properties. The reservoir space was subsequently expanded by karstification. Although the existence of hydrothermal fluid dolomitization in deep-burial environments has been accepted by many researchers (Zhu et al., 2009; Dong et al., 2013; Jin & Yu, 2011; Cai et al., 2001, 2009), there are few relevant reports about the developmental model of magmatic hydrothermal fluids. Therefore, the purpose of this article is to establish the identifying characteristics of deep hydrothermal fluid activity and to analyze the developmental model of magmatic hydrothermal fluids.

2. GEOLOGICAL SETTING

The Tarim Basin of Northwest China is a composite basin that formed from several distinct prototype basins (Tang et al., 2000), and it is the largest interior petroliferous basin in China. The basin can be divided into seven principal structural units (Fig. 1): the Tabei uplift (North Tarim), the Central uplift, the Southeast uplift, the Kuqa depression, the North depression, the Southwest depression, and the Southeast depression (Kang & Kang, 1996; Wei et al., 2000).

The present study area is located on the central uplift of the central Tarim Basin area and is a large, inherently low uplift consisting of platform carbonates overlying Carboniferous clastic rocks. The uplift was formed in the Ordovician, further developed in the Silurian–Devonian, and attained its existing shape in the Late Devonian. Ordovician sediments in this area were deposited on a platform and are now deeply buried (>5000 m burial depth; Fig. 1). The main rock types in the study area are limestone, dolomite, and evaporites. The Ordovician carbonate reservoir in the study area is subdivided into six formations: the Penglaiba (O1p), Yingshan (O1y), Yijianfang (O2yj), Qiaerbake (O3q), Lianglitage (O3l), Sangtamu (O3s), and Yijianfang (O2yj) formations (the latter is missing throughout most of the study area). The Penglaiba (O1p), Yingshan (O1y), and Lianglitage (O3l) formations, which are the focus of this study, consist of wackestones and packstones (Zhang et al., 2000; Ruan et al., 2013).

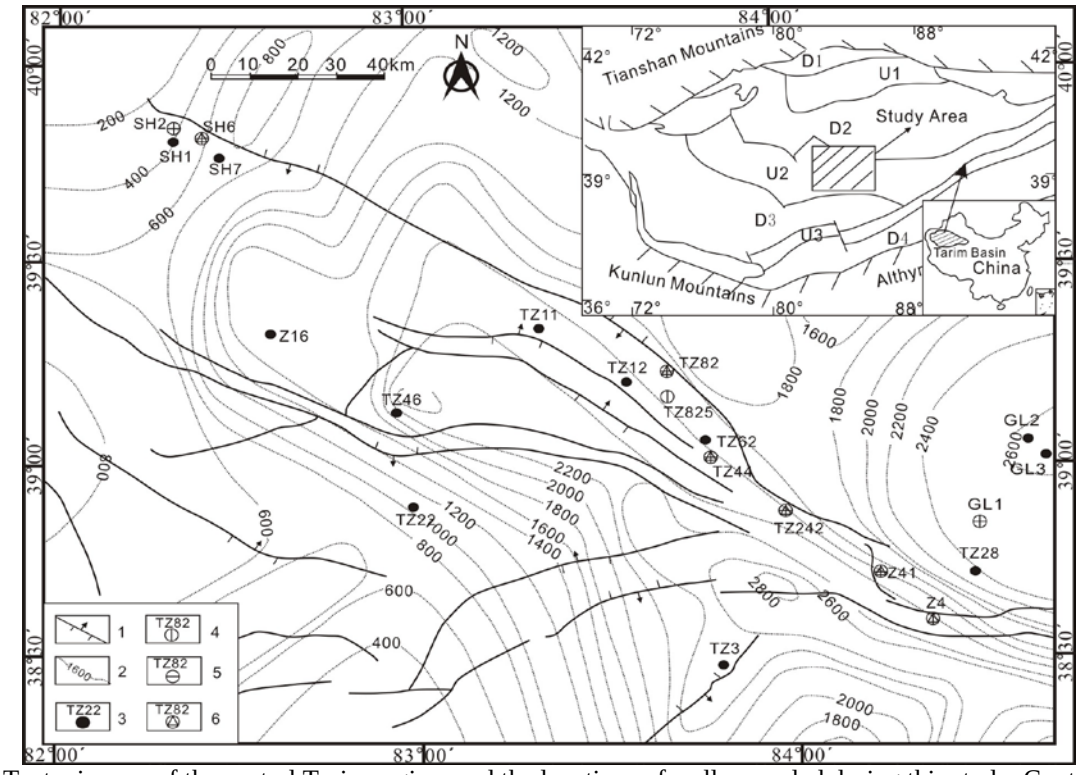

Figure 1. Tectonic map of the central Tarim region, and the locations of wells sampled during this study. Contours indicate the sedimentary topography before the Middle Ordovician. U1 = Tabei Uplift; U2 = Central Uplift; U3 = Southeast Uplift; D1 = Kuqu Depression; D2 = North Depression; D3 = Southwest Depression; D4 = Southeast Depression; 1 = Fault; 2 = Paleogeomorphology contours; 3 = Well location in study area; 4 = Sampled wells listed in Table 1; 5 = Sampled wells listed in Table 2; 6 = Sampled wells listed in Table 3.

Many faults are present in the study area and most strike NW–SE, converging toward the east. This fault system mainly consists of the central I fracture, the central II fracture, the TZ5 fracture and other fractures. In this fault system, the central I fracture controls sedimentary deposition, trap formation, oil and gas accumulation. Furthermore, the Ordovician carbonate reservoirs contain many tectonic fractures oriented NE–SW. These fractures formed mainly in the late Caledonian to early Hercynian, late Hercynian to Indosinian (257-205Ma), and Yanshanian (199.6-133.9Ma) to Neo-Alpine orogenesis (Liu et al., 2010). These fractures are generally planar and are commonly filled by pyrite, calcite, and other minerals. The area contains multiple unconformities, such as the unconformity between the Lower–Middle Ordovician and the Upper Ordovician. The development of these fault systems and unconformities provided a series of migration pathways for deep fluids.

3. SAMPLING AND ANALYTICAL METHODS

A number of cores have been recovered from drill-holes in Ordovician strata of the Tarim Basin (e.g., wells TZ242, TZ44, Z41, and SH2). The cores reveal numerous dissolution holes and fractures in the Ordovician carbonate reservoirs, and most of these are filled or partially filled by calcite, dolomite, pyrite, barite, and other minerals. To investigate the fluid type in the Ordovician carbonate reservoir during burial, filled carbonate or minerals (pyrite, gypsum) were chosen for analyses of trace elements, and carbon, oxygen, and strontium isotopes. Samples of country rock were also analyzed for comparison. Three separate batches of core samples were analyzed (Fig. 1).

The first 43 samples were selected from 11 wells (Fig. 1). These samples were ground to a powder (<200 mesh) for carbon and oxygen isotope analysis using a mass spectrometer (Mat252). The second 25 samples, selected from 8 wells (Fig. 1), were also ground to a powder (<200 mesh) for strontium isotope analysis. Mass-spectrometric analysis was performed at the China Nuclear Industry Institute, Peking, China. The $^{87}Sr/^{86}Sr$ values are corrected in accordance with the fractionation quality standards of $^{87}Sr/^{86}Sr = 0.1194$. The mean strontium isotopic value of the NBS987 standard sample is 0.710273 ± 0.000012, and the error is less than 2σ. In addition, 34 carbonate core samples were selected from 9 wells (Fig. 1), all of which were analyzed for trace elements and rare earth elements (REE) at the State Key Laboratory of Geological Process and Mineral Resources, Peking, China. Major elements were determined by XRF3080E at the China Nuclear Industry Institute, Peking, China. The rare earth elements were determined by ICP–MS while Sr and Ba were detected by (IRIS) ICP–AES.

We also obtained the temperatures of 408 fluid inclusions from 19 samples of fill material (from 10 wells). Fluid inclusion microthermometry using 0.2mm-thick doubly polished thin sections was undertaken using a Linkham THMSG600 heating–freezing stage with an automated controller unit, at China University of Geosciences, Peking, China. The initial heating rate was 15°C/min after temperature correction, and this was reduced to 1°C/min when the inclusion bubbles became smaller and more uniform. The measurement accuracy was ±1°C.

4. RESULTS AND DISSCUSSION

4.1 Petrology of Ordovician carbonate rock

Carbonate rocks in the study area are dominated by limestones that are subdivided into grainstones, micrites, dolomitic and algal limestones, and biolithites. Grainstones and micrites form 32.9% and 49.9% of the reservoir rocks in the study area, respectively. The porosity of the Ordovician limestone is generally <2.5%, with a range of 0.1%–8.63% and a mean value of 1.15%. Permeability is generally less than $10 \times 10^{-3}\mu m^2$, with an average of $3.31 \times 10^{-3}\mu m^2$. The porosity of less than 1% of the samples accounted for 36% of the total porosity, and the porosity of 50% samples is less than 1.14%, indicating the porosity of the original sedimentary limestone was low. The main reservoir space is dominated by various secondary dissolution pores that formed by karstification and dissolution by deep hydrothermal fluids. Such fluids often penetrate slowly along intercrystal pore sutures and micro-cracks to dissolve the country rock, thereby expanding intercrystal holes and improving the reservoir porosity and permeability. The main associated precipitation minerals include calcite, fluorite, pyrite, asphalt, clay, and dolomite (Fig. 2). Therefore, dissolution pores and the presence of precipitation minerals are important in terms of reservoir quality.

4.2. Temperature of fluid inclusions

Calcite fillings are widespread in Ordovician carbonate rocks in the central Tarim region, and the origins of the fillings are complex and diverse,

including atmospheric precipitation, ground water, and deep hydrothermal fluid. In this study, 18 wells were selected for microscopic examination and analysis of fluid inclusions, revealing a strip distribution of 4×4 to 10×12 (μm^2) or occasionally denser at 2×2 to 5×6 (μm^2). Most of the inclusions have a regular shape and the gas–liquid ratios are less than 5%. The homogenization temperatures of the fluid inclusions vary from 83°C to 166°C with a peak interval at 95°C–135°C; liquid is the homogeneous phase (Fig. 3).

According to the geothermal burial history and previous data (Cai et al., 2001), the maximum temperature of the Ordovician formation did not exceed 120°C. Therefore, if the homogenization temperature of the inclusions in Ordovician filling is >125°C, the formation of the filling can be attributed to hydrothermal fluids. The results show that many of the homogenization temperatures are above 125°C, up to a maximum of 298.9°C. These high-temperature inclusions provide important evidence for the influence of deep hydrothermal fluids.

4.3. Strontium, carbon, and oxygen isotopes

The results of carbon and oxygen isotope analyses are shown in Table 1. The $\delta^{13}C$ PDB values of the carbonate country rock range from –2.43 to 2.58, $\delta^{18}O$ PDB values range from –9.15 to 4.34, and the $\delta^{18}O$ (SMOW) values range from 21.43 to 26.39. The $\delta^{13}C$ PDB values of the filling samples range from –2.62 to 2.74, the $\delta^{18}O$ PDB values range from –15.18 to –4.23, and the $\delta^{18}O$ (SMOW) values from 15.21 to 26.5. The range of carbon and oxygen isotope values from the filling samples is greater than that of the country rock samples, highlighting the complexity of the fluid–rock interaction.

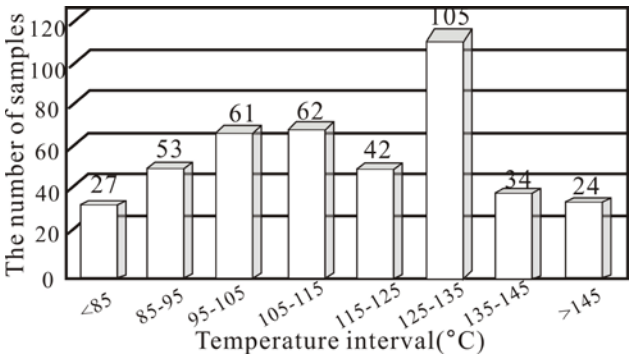

Figure 3. Frequency histograms of inclusion temperatures in filling material

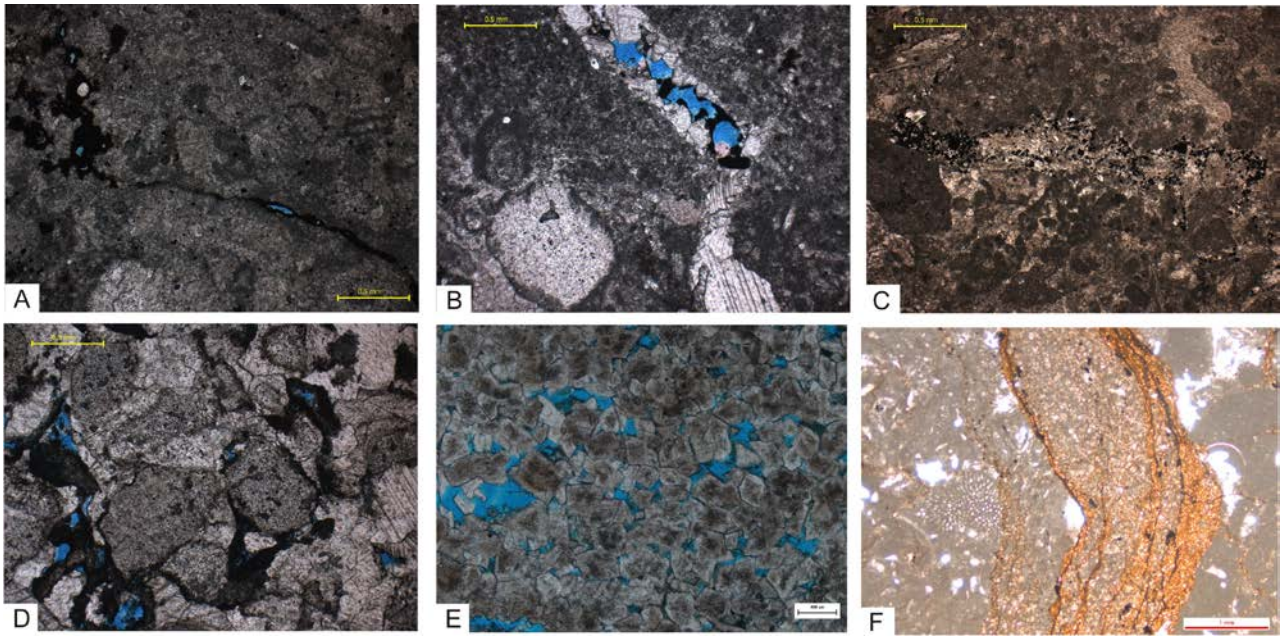

Figure 2. Dissolution and filling phenomenon in Ordovician carbonate rocks in the study area
A. Well GL1, 5876.18 m, cryptite, the dissolution seam is partially filled by asphalt and surrounded by pyrite (plane polarized light, sample O2y). B. Well Tz44, 4884.76 m, bioclastic wackestone, the dissolution seam is filled by calcsparite (plane polarized light, O3l). C. Well Tz408, 4582.53 m, uncharged dissolution seam in finely ashy crystalline dolomite (plane polarized light, O1p). D. Well Tz62, 5125.99 m, intergranular pores in grainstone are partly filled with clay and asphalt (plane polarized light, O3l). E. Well Z13, 5980.29 m, uncharged intergranular pore in finely crystalline dolomite (plane polarized light, O1y). F. Well Tz12, a structural dissolution seam in bioclastic wackestone is filled with asphalt and hydrothermal dolomite (plane polarized light, O2yj).

Table 1. Carbon and oxygen isotope compositions of country rock and fill material in the central Tarim Basin

samples	$\delta^{13}C$(PDB)‰	$\delta^{18}O$(PDB)‰	$\delta^{18}O$(SMOW)‰	Depth/m	Layer	litos	samples	$\delta^{13}C$(PDB)‰	$\delta^{18}O$(PDB)‰	$\delta^{18}O$(SMOW)‰	Depth/m	Layer	litos
SH6-4-2/57F	2.67	-9.1	21.48	6700.3	O3l	calcite matrix	TZ825-7K	2.15	-4.23	26.5	5431.69	O3l	crystalline limestone
SH 6-4-2/57W	2.55	-5.03	25.67	6700.3	O3l	oosparite	TZ825-7W	2.1	-4.34	26.39	5431.69	O3l	bioclastic limestone
SH 6-4K	2.25	-7.83	22.79	6653.42	O3l	crystalline limestone	Z41-4F	1.16	-4.8	25.91	6114.33	O3l	calcite matrix
SH 6-4W	2.58	-6.41	24.25	6653.42	O3l	bioclastic limestone	Z41-4W	1.08	-4.95	25.75	6114.33	O3l	bioclastic limestone
SH 6-5K	2.74	-8.38	22.22	6707.8	O3l	crystalline limestone	Z4-3-33/40K	1.2	-9.43	21.14	4521.5	O3l	crystalline limestone
SH 6-5W	2.49	-5.23	25.47	6707.8	O3l	crystalline limestone	Z4-3-33/40W	0.33	-8.7	21.9	4521.5	O3l	bioclastic limestone
TZ242-10K	0	-7.77	22.85	4537.29	O3l	crystalline limestone	GL1-2F	0.29	-12.74	17.73	5876.18	O2yj	calcite matrix
TZ242-10W	0.71	-5.27	25.43	4537.29	O3l	crystalline limestone	GL1-2W	0.87	-9.15	21.43	5876.18	O2yj	bioclastic limestone
TZ242-13F	1.31	-8.13	22.48	4753.4	O3l	calcite matrix	SH2-10-4/44K	2.35	-7.29	23.34	6876.5	O2yj	crystalline limestone
TZ242-13W	1.17	-5.28	25.41	4753.4	O3l	cryptite	SH2-10-4/44W	2.58	-4.53	26.19	6876.5	O2yj	grainstone
TZ242-1F	1.1	-6.64	24.01	4502.7	O3l	calcite matrix	SH2-4F	2.22	-15.18	15.21	6879.31	O2yj	calcite matrix
TZ242-1W	2	-5.83	24.85	4502.7	O3l	grainstone	SH2-4W	2.48	-6.53	24.12	6879.31	O2yj	bioclastic limestone
TZ44-1K	-0.32	-10.65	19.88	4838.26	O3l	crystalline limestone	SH2-9-9/55K	1.87	-7.62	23	6793.73	O2yj	crystalline limestone
TZ44-1K（i)	0.96	-12.39	18.09	4838.26	O3l	crystalline limestone	SH2-9-9/55W	2.36	-4.57	26.14	6793.73	O2yj	algal limestone
TZ44-1K(o)	-0.58	-10.57	19.96	4838.26	O3l	crystalline limestone	Z41-7F	-0.01	-7.09	23.55	6351.26	O2yj	calcite matrix
TZ44-1W	0.47	-6.33	24.33	4838.26	O3l	bioclastic limestone	Z41-7red	0.45	-5.77	24.92	6351.26	O2yj	crystalline limestone
TZ44-5-4/55W	0.78	-7.05	23.59	4880	O3l	bioclastic limestone	Z41-7W	0.28	-5.48	25.21	6351.26	O2yj	crystalline limestone
TZ44-5-4/55K	0.43	-10.02	20.53	4880	O3l	crystalline limestone	GL1-6F	-2.62	-11.88	18.61	6536.13	O1p	Calcite matrix
TZ44-4F	0.7	-9.49	21.08	4884.76	O3l	Calcite matrix	GL1-6W	-2.35	-6.91	23.74	6536.13	O1p	crystalline dolomite
TZ44-4W	0.68	-6.85	23.8	4884.76	O3l	bioclastic limestone	TZ82-4K	0.89	-7.58	23.04	5365.24	O3l	crystalline limestone
TZ82-15-2/21K	1.07	-8.47	22.13	5481.28	O3l	crystalline limestone	TZ82-4W	1.25	-5.76	24.92	5365.24	O3l	grainstone
TZ82-15-2/21W	1.63	-5.56	25.13	5481.28	O3l	cryptite							

Previous studies of carbon and oxygen isotopes in carbonate provide a solid basis for our research, although controversy exists regarding the range of isotope values in mantle carbonatites and sedimentary carbonates (< ±1‰) (Bas et al., 1997; Demeny et al., 1998; Keller & Hoefs, 1995; Valley, 1986; Zheng & Chen, 2000). From the literature, it is clear that carbonates with lower carbon and oxygen isotope values formed in a high-temperature environment, particularly for the lower $\delta^{18}O$ PDB values (Zheng & Chen, 2000). The accumulation of magmatic hydrothermal energy appears to increase the temperature. Valley (1986) concluded that carbon and oxygen isotopic values are influenced by the composition of the original rock, fluid type, fluid/rock ratio, temperature history, and many other factors. Land & Hoops (1973) suggested that the lower the $\delta^{18}O$PDB value in carbonate rocks, the higher the carbonate formation temperature. Therefore, lower $\delta^{18}O$PDB values in filling carbonate may indicate high-temperature fluid activity. The results of the carbon and oxygen isotope analyses are shown in figure 4.

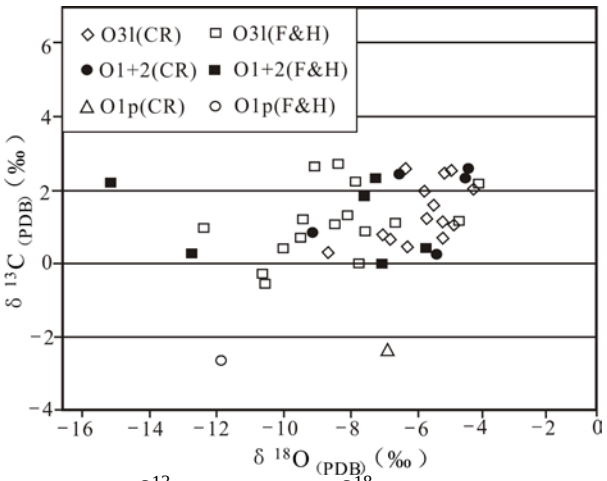

Figure 4. $\delta^{13}C$ PDB versus $\delta^{18}O$ PDB content in Ordovician strata in the study region

In figure 2, carbon and oxygen isotope values of country rocks show a tightly clustered distribution. The $\delta^{18}O$ PDB values range from −10 to −4, while the $\delta^{13}C$ PDB values range from 0 to 2.6, with the exception of one point, which represents a standard of normal sedimentary carbonate in seawater. The carbon and oxygen isotopic values from most of the fill samples are similar to the values found in the country rocks (e.g., wells TZ82, Z4, and SH2). This indicates formation in a normal fluid. On the other hand, the carbon and oxygen isotope values from several filling samples are distinct from those observed in the country rock. $\delta^{18}O$ PDB values are <10 (e.g., samples from Wells TZ44 and GL1), indicating a high-temperature environment during the formation of these samples, possibly related to magmatic hydrothermal activity.

Table 2 lists the results of strontium isotope analyses of 25 samples (8 wells). The $^{87}Sr/^{86}Sr$ values of the carbonate country rock samples range from 0.708228 to 0.709114, with a mean value of 0.7086 and a maximum of 0.709675. The $^{87}Sr/^{86}Sr$ values for the filling samples range from 0.70812 to 0.709853, with a mean value of 0.708950 and a maximum of 0.709853.

The strontium isotopes in depositional carbonate are controlled mainly by the properties of oceanic/lacustrine water, while the strontium isotopes in carbonate cements are influenced by groundwater or diagenetic fluids (Land & Hoops, 1973). The results of strontium isotope analyses of the Ordovician carbonate rock are consistent with results from previous reports (e.g., Denison et al., 1998). Some of the $^{87}Sr/^{86}Sr$ values, (e.g., samples from Wells TZ82 and Z41) are <0.709, which is similar to the country rock values, indicating a normal sedimentary environment. The $^{87}Sr/^{86}Sr$ values from the other sample set are higher (>0.709) (Fig. 5).

Felsic rocks and mudstone have relatively high $^{87}Sr/^{86}Sr$ values, with high amounts of radiogenic ^{87}Sr (Winter et al., 1997). In addition, hydrothermal fluids related to acidic volcanic and magmatic processes usually contain more radiogenic ^{87}Sr, causing the fillings to yield higher $^{87}Sr/^{86}Sr$ values (Yang, 1988). The higher $^{87}Sr/^{86}Sr$ values of Ordovician fillings were possibly controlled by atmospheric precipitation and the subsequent dissolution related to atmospheric water in the Tarim Basin, especially in the northern part of the basin (Zhang & Cai, 2007).

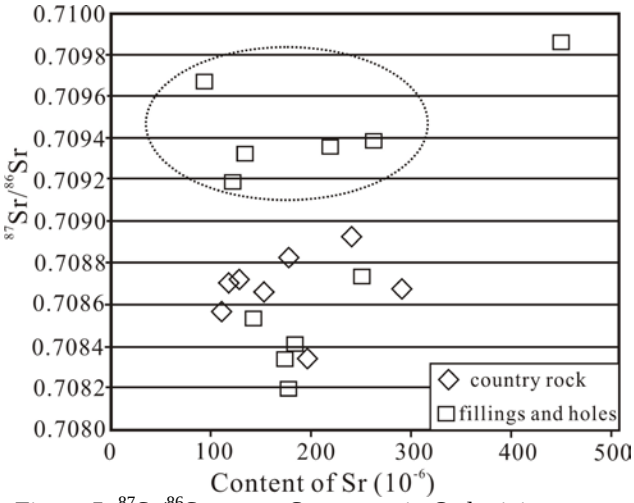

Figure 5. $^{87}Sr/^{86}Sr$ versus Sr content in Ordovician strata in the study region.

Table 2. Strontium isotope compositions of country rock and filling samples in the central Tarim Basin

Samples	Depth/m	$^{87}Sr/^{86}Sr$	Layer	Lithos	Samples	Depth/m	$^{87}Sr/^{86}Sr$	Layer	Lithos
TZ44-5-4/55K	4890.02	0.709185	O3l	limestone	Z41-4F	6114.33	0.708402	O2yj	limestone
TZ44-5-4/55W	4890.02	0.708577	O3l		Z41-4W	6114.33	0.708843	O2yj	
TZ44-1K(inside)	4838.26	0.709853	O3l		Z41-7F	6114.33	0.708732	O2yj	
TZ44-1K(outside)	4838.26	0.709383	O3l		Z41-7W	6114.33	0.708673	O2yj	
TZ44-1W	4838.26	0.709114	O3l		SH2-9-9/55K	6793.73	0.70812	O3l	
TZ44-4F	4838.26	0.709332	O3l		SH2-9-9/55W	6793.73	0.708572	O3l	
TZ44-4W	4838.26	0.708714	O3l		SH6-4-2/57F	6700.3	0.708537	O3l	
TZ82-15-2/21K	5481.28	0.708336	O3l		SH6-4-2/57W	6700.3	0.708659	O3l	
TZ82-15-2/21W	5481.28	0.708353	O3l		T1-4K	2265.65	0.709244	O3l	
TZ242-1F	4537.29	0.709363	O3l		T1-4W	2265.65	0.708278	O3l	
TZ242-1W	4537.29	0.708726	O3l		GL1-2F	6536.13	0.709675	O2yj	
TZ242-13F	4753.4	0.708187	O3l		GL1-2W	6536.13	0.708228	O2yj	
TZ242-13W	4753.4	0.708942	O3l						

4.4. Trace elements

Trace element and rare earth element analyses of 11 fillings samples (6 wells) revealed 43 individual elements. Ba had the highest concentration of 16,178 ppm (Table 3). Trace amounts of Re were found, while Ba, Sr, V occurred at concentrations of ~10 ppm. The mass fraction of rare earth elements in the fillings varied spatially, from 0.012–9.37 ppm. The value of δEu in most of the samples was limited to 0.556–0.981 with the exception of samples TZ44-1(I) and TZ44-1(O). A REE distribution map shows a consistent trend of REE alteration (Fig. 6), while δEu showed significant positive anomalies in samples TZ44-1(I) and TZ44-1(O).

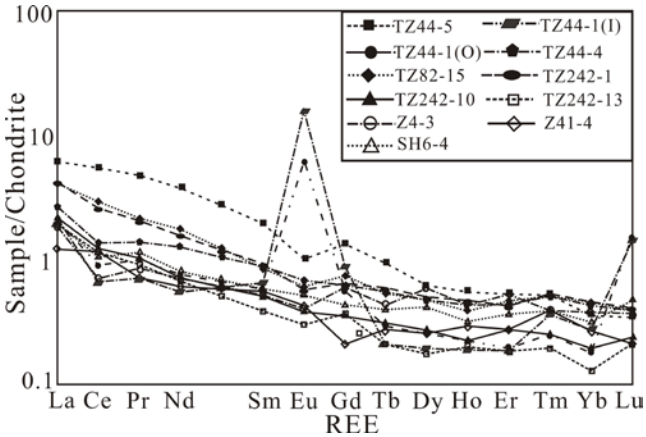

Figure 6. Chondrite-normalized REE patterns for filling samples from the central Tarim region

The radius of Ba^{2+} is too large to enter the crystal lattice of carbonate rocks, meaning that the Ba content of normal sedimentary carbonate is generally low. Carbonate minerals that precipitate from Ba-rich hydrothermal fluids have a much higher Ba content (Cai et al., 2009). It is therefore inferred that the Ba-enriched samples indicate formation in a hydrothermal fluid environment.

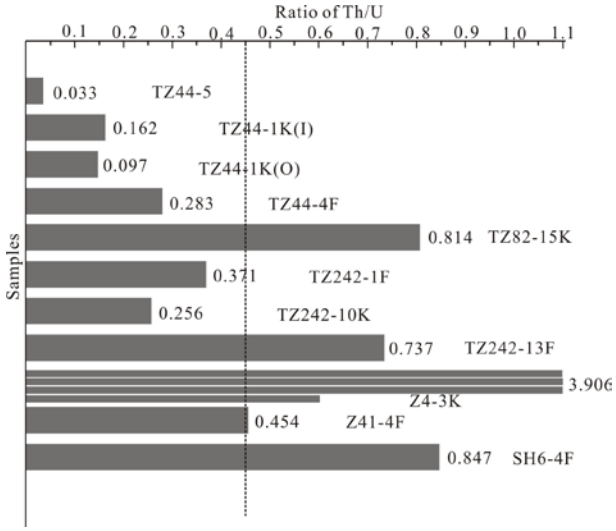

Figure 7. Values of U/Th for filling samples from the central Tarim region

U is enriched in the mantle whereas Th and O contents decrease with depth. Therefore, the Th/U ratio is not only representative of redox conditions, but also the fluid source. A lower Th/U ratio indicates greater proximity to the mantle-sourced fluid. The Th/U ratio of country carbonate rocks in the present study area is 0.91, which is significantly lower than the average crustal value of 3.56 (Taylor, 1964), and is close to the value of 0.78 for carbonate rocks reported by Turekian & Wedepohl (1961). The U/Th values in filled calcite are lower than that of the country carbonate rocks (Fig. 7).

Table 3. Abundance of trace elements in filling samples from the central Tarim Basin (ppm)

Samples	Be	Sc	V	Cr	Co	Ni	Cu	Zn	Ga	Rb	Sr	Y	Nb	Mo	Cd	In	Sb	Cs	Ba	La	Ce	Pr
TZ44-5-4/55K	0.442	0.307	28	1.38	0.57	5.98	1.84	3.03	0.343	1.94	123	1.4	0.126	0.591	0.02	0.004	0.103	0.083	35	0.722	0.999	0.157
TZ44-1K(I)	0.386	0.591	18.2	2.06	0.631	13.7	3.6	11.8	0.338	1.01	451	1.42	0.105	0.619	0.142	0.002	0.094	0.047	16178	0.793	0.635	0.098
TZ44-1K(O)	0.596	0.545	17.1	1.5	0.584	9.36	2.24	18.5	0.332	0.621	263	1.23	0.05	0.485	0.175	0.002	0.118	0.033	6589	0.766	0.866	0.137
TZ44-4F	0.593	0.678	23.3	5.98	1.03	8.79	1.79	3.11	0.436	0.711	136	2.08	0.299	0.522	0.012	0.002	0.103	0.019	44.6	0.986	1.3	0.189
TZ82-15K	0.358	0.774	20.4	2.52	1.25	7.28	2.65	6.38	0.713	3.37	174	1.24	0.413	0.441	0.013	0.003	0.096	0.146	21.2	1.49	2.8	0.295
TZ242-1F	0.568	0.324	21.5	3.11	0.579	5.23	0.973	3.19	0.415	0.433	220	2.29	0.028	0.321	0.028	0.003	0.035	0.007	34.4	0.679	0.677	0.117
TZ242-10K	0.411	0.427	23.1	1.35	0.496	5.52	0.752	7.39	0.403	0.394	132	1.17	0.01	0.324	0.093	0.002	0.033	0.008	10.8	0.799	1.17	0.142
TZ242-13F	0.566	0.444	23.6	0.851	0.499	5.49	1.05	2.79	0.394	0.518	177	0.648	0.073	0.401	0.026	0.004	0.082	0.021	14.1	0.714	1.1	0.125
Z4-3K	0.784	1.66	23.6	6.28	1.78	7.99	3.61	53.1	2.23	16.6	193	5.46	1.76	0.394	0.032	0.006	0.132	0.751	226	5.86	9.37	1.06
Z41-4F	0.246	0.498	17.2	0.665	1.73	8.07	2.8	83.9	0.391	1.52	185	0.783	0.139	0.883	0.067	0.004	0.134	0.045	198	0.445	1.11	0.098
SH6-4F	0.534	0.636	8.66	2.16	0.901	5.83	1.2	4.17	0.237	0.475	142	2.64	0.066	0.313	0.006	0.002	0.033	0.007	149	3.39	7.9	0.986
Samples	**Nd**	**Sm**	**Eu**	**Gd**	**Tb**	**Dy**	**Ho**	**Er**	**Tm**	**Yb**	**Lu**	**Ta**	**W**	**Re**	**Tl**	**Pb**	**Bi**	**Th**	**U**	**Zr**	**Hf**	**δCe**
TZ44-5K	0.568	0.134	0.045	0.133	0.023	0.157	0.027	0.09	0.014	0.078	0.018	0.018	0.147		0.049	1.35	0.031	0.234	7.01	1.69	0.051	0.924
TZ44-1K(I)	0.39	0.152	1.38	0.268	0.012	0.074	0.016	0.046	0.013	0.067	0.055	0.069	0.152	0.002	0.055	6.12	0.011	0.315	1.94	0.883	0.017	19.200
TZ44-1K(O)	0.542	0.132	0.547	0.17	0.017	0.098	0.019	0.048	0.009	0.044	0.06	0.021	0.063	0.002	0.035	12.8	0.026	0.167	1.72	0.649	0.019	10.22
TZ44-4F	0.895	0.203	0.059	0.189	0.032	0.181	0.037	0.109	0.018	0.106	0.015	0.86	0.163	0.001	0.096	2.34	0.031	0.292	1.03	1.9	0.049	0.819
TZ82-15K	1.25	0.198	0.053	0.228	0.031	0.181	0.033	0.116	0.018	0.113	0.015	0.066	0.153	0.001	0.058	2.35	0.031	0.57	0.7	5.88	0.159	0.693
TZ242-1F	0.498	0.12	0.035	0.183	0.025	0.225	0.037	0.13	0.014	0.094	0.014	0.01	0.056	0.001	0.049	3.47	0.039	0.235	0.633	0.445	0.006	0.664
TZ242-10K	0.504	0.117	0.033	0.108	0.018	0.104	0.019	0.068	0.009	0.048	0.009	0.008	0.031		0.043	5.97	0.019	0.11	0.429	0.326	0.006	0.797
TZ242-13F	0.476	0.089	0.026	0.111	0.012	0.067	0.017	0.046	0.007	0.032	0.008	0.013	0.057	0.001	0.002	0.916	0.02	0.16	0.217	1.79	0.04	0.731
Z4-3K	4.19	0.811	0.188	0.749	0.132	0.731	0.152	0.403	0.072	0.435	0.059	0.143	0.213		0.104	6.95	0.032	2.5	0.64	30.6	0.855	0.655
Z41-4F	0.433	0.128	0.037	0.065	0.016	0.098	0.025	0.068	0.014	0.066	0.008	0.019	0.079	0.002	0.077	3.22	0.013	0.248	0.546	1.59	0.041	0.981
SH6-4F	4.12	0.68	0.133	0.618	0.082	0.36	0.071	0.199	0.028	0.133	0.02	0.084	0.113		0.008	0.711	0.024	0.188	0.222	0.447	0.004	0.556

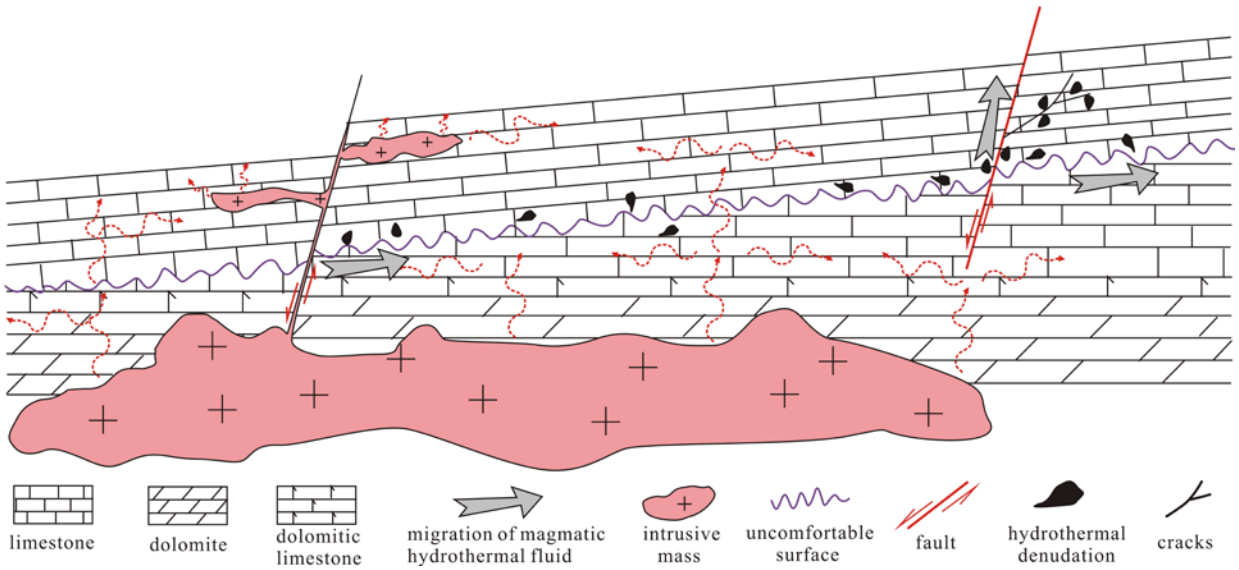

Figure 8. Model of deep hydrothermal fluid for Ordovician carbonate rock in the central Tarim region.

Two possible mechanisms may explain the low U/Th ratio. 1) The impact of reducing depositional or mantle-derived fluids is potentially important, as samples with a U/Th value of <0.45 are inferred to be directly related to mantle-derived magmatic fluid. 2) Higher Th/U values in fractured filling in well Z41 are indicative of the influence of clay-rich fluid from the weathering crust between Late Cambrian and Early Ordovician strata.

4.5. Origin of magmatic hydrothermal fluids

Large amounts of volcanic rock occur in sedimentary formations in the central Tarim region, and the multi-stage nature of volcanic activity has become apparent during exploration for oil and gas, although the number of stages remains debated (Li et al., 2005, Li et al., 2007, Zhang et al., 2003). Chen et al., (2006) noted that Permian volcanic rocks in Tarim basin cover $>2 \times 10^5$ km^2 and 32 exploration wells have reached the volcanic rock.

Given the abundance of volcanic rocks in the study area, the buried dissolution in Ordovician carbonate rocks may have been related to a magmatic hydrothermal fluid, as supported by the fluorite and barite fillings found in holes and cracks. However, the present study found that the magmatic hydrothermal activity is not as widespread as previously thought, as inferred from an analysis of C, O, and Sr isotopes and trace elements. The observed characteristics of the filling are very similar to those of normal carbonate rock (e.g., samples from Wells SH6, Z4, TZ82, and Z41). Only a few samples sourced from close to major faults show characteristics indicative of magmatic hydrothermal fluid (e.g., Wells GL1 and TZ44). Hydrothermal fluid does not necessarily affect the whole vertical section in a given core, as shown by the fact that sample TZ242-1F has been altered by magmatic hydrothermal fluids, whereas sample TZ242-13F, from the same core but a different depth, shows no such alteration.

Based on the above results, a model of deep hydrothermal fluid is proposed for Ordovician carbonate rock in the study area (Fig. 8). The volcanic history of the basin involved two stages. First, heat from the magma caused thermal metamorphism of the carbonate rocks, leading to the recrystallization of dolomite in Lower Ordovician layer and the heating of formation fluids. Second, the hydrothermal fluid migrated along unconformities, faults, and fractures during the late stage of volcanic activity, resulting in dissolution and filling. The migration of such fluids is limited both vertically and horizontally, and migration requires pre-existing pathways.

5. CONCLUSIONS

Ordovician carbonate reservoirs of the central Tarim region contain many subsurface dissolution and filling phenomena that may be related to late-stage deep magmatic activity. The isotopic study of filling and country carbonate rocks shows a bimodal distribution of values, with some samples having low $\delta^{13}C$ and $\delta^{18}O$ values (e.g., TZ44-1K, TZ44-5K, SH2-4F, and GL1-2F) and some having high $^{87}Sr/^{86}Sr$ values (TZ44-1K, TZ44-5K, TZ242-1F, and GL1-2F). The isotope values obtained for these samples are different from those for other filling and country rock samples. Trace element analysis of the filling samples shows positive Eu anomalies and

high Th/U values, indicating the influence of magmatic hydrothermal fluids. The migration of such fluids is limited both vertically and horizontally by the extent of fault and fracture systems. Magmatic activity has the further effect of heating the formation fluid, which resulted in the formation of many high-temperature fluid inclusions.

ACKNOWLEGMENTS

This study was financially supported by funds from the Chinese National 973 Program (20011CB201100-03, 2006CB202302) and Chinese National Oil and Gas Program (2011ZX05005-004-HZ06，2011ZX05009-002-402).

REFERENCES

Al-Aasm, I., 2003. *Origin and characterization of hydrothermal dolomite in the Western Canada sedimentary basin*. Journal of Geochemical Exploration. Journal of Geochemical Exploration, 78-79: 9-15.

Auajjar, J. & Boulègue, J., 2002. *Dolomites in the Tazekka Pb-Zn district, eastern Morocco: polyphase origin from hydrothermal fluids*. Terra Nova, 14:175-182.

Barnes, D.A., Parris, T.M. & Grammer, G.M., 2008. *Hydrothermal dolomitization of fluid reservoirs in the Michigan basin, U.S.A. In: 2008 AAPG Annual Convention & Exhibition*. Abstracts Volume, Anonymous, 2-3.

Bas, M.J.L., Spiro, B. & Yang, X.,1997. *Oxygen, carbon and strontium isotope study of the carbonatitic dolomite host of the Bayan Obo Fe-Nb REE deposit, InnerMongolia, North China*. Mineralogical Magzine, 61:531-541.

Cai, C., Hu, W. & Worden, R.H., 2001. *Thermochemical sulphate reduction in Cambrain-Ordovician carbonates in Central Tarim*. Marine and Petroleum Geology, 18(6): 729-741.

Cai, C.F., Zhang, C.M., Cai, L.L., Wu, G.H., Jiang, L., Xu, Z.M., Li, K.K. & Ma, A.L., 2009. *Origins of Palaeozoic oils in the Tarim Basin: Evidence from sulfur isotopes and biomarkers*. Chemical Geology, 268:197-210.

Chen, H.L., Yang, S.F., Wang, Q.H., Luo, J.C., Jia, C.Z., Wei, G.Q., Li, Z.L., He, G.Y. & Hu, A.P., 2006. *Sedimentary response to Early-Mid Permian basaltic magmatism in the Tarim plate*. Geology in China, 3:545-552 (in Chinese with English abstract).

Chen, Z.Y., Yan, H., Li, J.S., Ge, Z., Zhang, Z.W. & Liu, B.Z., 1999. *Relationship Between Teriary Volcanic Rocks and Hydrocarbons in the Liaohe Basin, People, Republic of China*. AAPG Bulletin, 83(6):1004-1014.

Davies, G.R. & Smith, L.B.Jr., 2006. *Structurally controlled hydrothermal dolomite reservoir facies: An overview*. AAPG Bulletin, 90:1641-1690.

Davies, G.R. & Smith, L.B.Jr., 2007. *Structurally controlled hydrothermal dolomite reservoir facies: An overview: Reply*. AAPG Bulletin, 91:1342-1344.

Demeny, A., Ahijado, A. & Casillas, R., 1998. *Crustal contamination and fluid/rock interaction in the carbonatites of Fuerteventura (Canary Island, Spain): a C, O, H isotope study*. Lithos, 44:101-115.

Denison, R.E., Koepnick, R.B., Burke, W.H. & Hetherington, E.A., 1998. *Construction of the Cambrian and Ordovician seawater n(^{87}Sr) /n(^{86}Sr) curve.* Chemical Geology,152 (3) : 325 -340 .

Dong, S., Chen, D.Z., Qing, H.R., Zhou, X.Q., Wang, D., Guo, Z.H., Jiang, M.S. & Qian, Y.X., 2013. *Hydrothermal alteration of dolostones in the Lower Ordovician, Tarim Basin, NW China: Multiple constraints from petrology, isotope geochemistry and fluid inclusion microthermometry*. Marine and Petroleum Geology, 46(0): 270-286.

Friedman, G.M., 2007. *Structurally controlled hydrothermal dolomite reservoir facies: An overview: Discussion*. AAPG Bulletin, 91:1339-1341.

Guedes, S.C., Rosière, C.A. & Barley, M.E., 2003. *The association of carbonate alteration of banded iron formation with the Carajás high-grade hematite deposits*. Applied Earth Science, 12:26-35.

James, P.R. & Mark, W.L., 2001. *An introduction to chert reservoirs of North America*. AAPG Bulletin, 85:1-5.

Jin, Z. & Yu, K., 2011. *Characteristics and significance of the burial dissolution of dolomite reservoirs: Taking the Lower Paleozoic in eastern Tarim Basin as an example*. Petroleum Exploration and Development, 38(4):428-435.

Jin, Z.J., Zhang, L.P., Yang, L. & Hu, W.X., 2004. *A preliminary study of mantle- derived fluids and their effects on oil/gas generation in sedimentary basins.* Journal of Petroleum Science & Engineering, 41: 45-56.

Kang, Y.Z. & Kang, Z.H., 1996. *Tectonic evolution and Oil and Gas of Tarim Basin*. J. Southeast Asian Earth Sci, 13:317-325.

Kappler, P. & Zeeh, S., 2003. *Relationship between fluid flow and faulting in the Alpine realm (Austria, Germany, Italy)*. Sedimentary Geology, 131:147-162.

Keller, J. & Hoefs, J., 1995. *Stable isotope characteristics of recent natrocarbonatite from Oldoinyo Lengai. In: Bell K, Keller J, eds. Carbonatite Volcanism: Oldoinyo Lengai and the Petrogenesis of Natrocarbonatite*. Berlin: Springer Verlag, 113-123.

Land, L.S. & Hoops, G.K., 1973. *Sodium in carbonate sediments and rocks: A possible index to the salinity of diagenetic solutions*. Journal of Sedimentary Petrology, 43:614-617.

Lavoie, D. & Morin, C., 2004. *Hydrothermal*

dolomitization in the Lower Silurian Sayabec Formation in northern Gaspé-Matap-édia (Québec): Constraint on timing of porosity and regional significance for hydrocarbon reservoirs. Bulletin of Canadian Petroleum Geology,52:256-269.

Lavoie, D. & Chi, G.X., 2006. *Hydrothermal dolomitization in the Lower Silurian La Vieille Formation in northern New Brunswick: Geological context and significance for hydrocarbon exploration*. Bulletin of Canadian Petroleum Geology, 54:380-395.

Li, Y., Su, W., Kong, P., Qian, Y.X., Zhang, K.Y., Zhang, M.L., Chen, Y., Cai, X.Y. & You, D.H., 2007. *Zircon U-Pb ages of the Early Permian Magmatic rocks in the Tazhong-Bachu region, Tarim basin by LA-ICP-MS*. Acta Petrologica Sinica, 23(5):1097-1107 (in Chinese with English abstract).

Li, Y.J., Song, W.J., Wu, G.Y., Wang, Y.F., Li, Y.P. & Zheng, D.M., 2005. *Jinning granodiorite and diorite deeply concealed in the central Tarim Basin*. Science in China Series D: Earth Science, 48(12): 2061-2068.

Liu, X.C., Li, T.G. & Liu, C.X., 2010. *Deep fluid activity in Central Tarim basin and its heating effects on hydrocarbon generation and accumulation.* Journal of Jilin University (Earth Science Edition), 40(2):279-285 (in Chinese with English abstract).

Machel, H.G. & Buschkuehle, B.E., 2008. *Diagenesis of the Devonian Southesk-Cairn carbonate complex, Alberta, Canada: Marine cementation, burial dolomitization， thermochemical sulfate reduction, anhydritization, and squeegee fluid flow*. Journal of Sedimentary Research, 78:366-389.

Ruan, Z., Yu, B.S., Wang, L.D., Pan, Y.L. & Tan, G.H., 2013. *Prediction of buried calcite dissolution in the Ordovician carbonate reservoir of the Tahe Oilfield, NW china: Evidence from formation water*. Chemie der Erde: geochemistry, 73: 469-479. In the text is 2012

Taylor, S.R., 1964. *Abundance of chemical elements in the continental crust: A new table*. G.C.A., 28, 1273-1285.

Tang, L.J., Jing, Z.J., & Pang, X.Q., 2000. *Hydrocarbon migration and accumulation models of superimposed basins.* Journal of the University of Petroleum, China (Edition of Natural Science), 24:418-426 (in Chinese with English abstract).

Tritlla, J., Cardellach, E. & Sharp, Z.D., 2001. *Origin of vein hydrothermal carbonates in Triassic limestones of the Espadan Ranges Iberian Chain, E Spain*. Chemical Geology, 172:291-305.

Turekian, K.K. & Wedepohl, K.H., 1961. *Distribution of the elements in major units of the earth crust*. Geological Society America Bulletin, 72:172-192.

Valley, J.W., 1986. *Stable isotope geochemistry of metamorphic rocks. In: Valley J H, Taylor H P J, O ' Neil J R, eds. Stable Isotopes in High Temperature Geological Processes*. Review of Mineralogy, 16:445-489.

Wei, G.Q., Jia, C.Z., Song, H.Z., Shi, Y.S., Liu, H.F. & Li, Y.H., 2000. *Ordovician structure depositional model and prediction of Profitable crack reservoir of carbonate rock in Tazhong area, Tarim basin*. Acta Sediment. Sin, 18: 408-413 (in Chinese with English abstract).

Winter, B.L., Johnson, C.M. & Clark, D.L., 1997. *Strontium, neodymium, and lead isotope variations of authigenic and silicate sediment components from the Late Cenozoic Arctic Ocean: Implications for sediment provenance and the source of trace metals in seawater*. Geochimica et Cosmochimica Acta, 61(19): 4181-4200.

Worden, R.H., Smalley, P.C. & Oxtoby, N.H., 1996. *Reply to the comment by H.G.MACHEL on "The effects of thermochemical sulfate reduction upon formation water salinity and oxygen isotopes in carbonate reservoirs"*. Geochim Cosmochim Acta, 62:343-346.

Worden, R.H. & Cai, C.F., 2006. *Geochemical characteristics of the Zhaolanzhuang sour gas accumulation and thermochemical sulfate reduction in the Jixian Sag of Bohai Bay basin: Discussion.* Organic Geochemistry, 37(4):511-514.

Yang, H., 1988. *The genesis , characteristics , distribution rule of the granite in the eastern Tianshan Mountain and it s relation to tectonic background and ore deposit*. 1 edition., Nanjing: Nanjing University (in Chinese).

Zhang, C.L., Zhao, Y., Guo, K.Y., Dong, Y.G. & Wang, A.G., 2003. *Geochemistry Characteristics of the Proterozoic Meta-Basalt in Southern Tarim Plate : Evidence for the Meso-Proterozoic Breakup of Paleo-Tarim Plate.* Earth Science-Journal of China University of Geosciences, 28(1): 47-53 (in Chinese with English abstract).

Zhang, S.C., Hanson, A.D., Moldowan, J.M., Graham, S.A., Liang, D.G., Chang, E. & Fago, F., 2000. *Paleozoic oil-source rock correlations in the Tarim basin, NW China. Org*. Geochem., 31:273-286.

Zhang, T.W., Amrani, A., Ellis, G.S., Ma, Q.S. & Tang, Y.C., 2008. *Experimental investiga-tion on thermochemical sulfate reduction by H_2S initiation*. Geochimica et Cosmochimica Acta, 72:3518-3530.

Zhang, T. & Cai, X.Y., 2007. *Caledonian paleokarstification and its characteristics in Tahe area , Tarim Basin*. Acta Geologica Sinica, 81(8): 1125-1134 (in Chinese with English abstract).

Zheng, Y. & Chen, J., 2000. *Stable Isotopic Geochemistry*. Beijing: Science Press.

Zhu, D.Y., Jin, Z.J. & Hu, W.X., 2009. *Hydrothermal alteration dolomite reservoir in Tazhong area*. Acta Petrol Ei Sinica, 30(5): 698-704.

Received at: 11. 06. 2014
Revised at: 02. 12. 2014
Accepted for publication at: 30. 01. 2015
Published online at: 10. 03. 2015